Equation of state of fully ionized electron-ion plasmas

Gilles Chabrier

Centre de Recherche Astronomique de Lyon, Centre National de la Recherche Scientifique UMR No. 5574,
Ecole Normale Supérieure de Lyon, 69364 Lyon Cedex 07, France

Alexander Y. Potekhin

Ioffe Physical-Technical Institute, 194021 St. Petersburg, Russia

Thermodynamic quantities of Coulomb plasmas consisting of pointlike ions immersed in a compressible, polarizable electron background are calculated for ion charges $Z = 1-26$ and for a wide domain of plasma parameters ranging from the Debye-Hückel limit to the crystallization point and from the region of nondegenerate to fully degenerate nonrelativistic or relativistic electrons. The calculations are based on the linear-response theory for the electron-ion interaction, including the local-field corrections in the electronic dielectric function. The thermodynamic quantities are calculated in the framework of the *N*-body hypernetted-chain equations and fitted by analytic expressions. We present also accurate analytic approximations for the free energy of the ideal electron gas at arbitrary degeneracy and relativity and for the excess free energy of the one-component plasma of ions derived from Monte Carlo simulations. The extension to multi-ionic mixtures is discussed within the framework of the linear mixing rule. These formulas provide a completely analytic, accurate description of the thermodynamic quantities of fully ionized electron-ion Coulomb plasmas, a useful tool for various applications from liquid state theory to dense stellar matter. [S1063-651X(98)03410-2]

PACS number(s): 52.25.Kn, 05.70.Ce

I. INTRODUCTION

Electron-ion plasmas (EIPs) consisting of different species of pointlike ions (charge $Z_i e$, mass $m_i = A_i$ amu) and electrons ($-e, m_e$) are encountered in numerous physical and astrophysical situations, e.g., inertially confined laboratory plasmas, liquid metals, stellar and planetary interiors, and supernova explosions [1]. Full ionization is reached either at high temperatures T and low densities ρ (thermal ionization) or at high enough densities ρ (pressure ionization). Even when these conditions are not satisfied, the approximation of full ionization is useful for calculations in the mean ion approximation, in which the mean ion charge corresponds to its partial ionization stage. On the other hand, the free energy of fully ionized EIP provides the reference system for models aimed at describing the thermodynamic properties of partially ionized plasmas [2]. In this paper we present a completely analytic model for the free energy of EIP, based on detailed numerical calculations for different ionic species Z over a wide range of density and temperature. We first focus on the two-component plasma (TCP), consisting of electrons and a single species of ions. An extension to ionic mixtures is considered in Sec. VI.

The Coulomb plasmas can be characterized by the electron coupling parameter Γ_e and the density parameter r_s,

$$\Gamma_e = \beta e^2 / a_e, \quad r_s = a_e / a_B, \qquad (1)$$

where $\beta = (k_B T)^{-1}$ is the inverse thermodynamic temperature, k_B is the Boltzmann constant, $a_e = (\frac{4}{3} \pi n_e)^{-1/3}$ measures the mean interelectron distance, n_e is the electron number density, and $a_B = \hbar^2 / m_e e^2$ is the Bohr radius. These parameters can be evaluated as $\Gamma_e \approx (2.693 \times 10^5 \text{ K}/T) n_{24}^{1/3}$ $= (23.2 \text{ eV}/k_B T) n_{24}^{1/3}$ and $r_s \approx 1.172 n_{24}^{-1/3}$, where n_{24}

$\equiv n_e / 10^{24}$ cm$^{-3} \approx (\rho / 1.6605 \text{ g cm}^{-3}) \langle Z \rangle / \langle A \rangle$. Here and hereinafter, $\langle X \rangle = \Sigma_i n_i X_i / \Sigma_i n_i$ denotes the average over all ions and n_i the number density of ions of ith species.

The ion coupling parameter of the TCP is

$$\Gamma_i = \beta (Ze)^2 / a_i = \Gamma_e Z^{5/3}, \qquad (2)$$

where a_i is the mean interionic distance ($a_i = a_e Z^{1/3}$ due to the electroneutrality condition $n_e = n_i Z$). In multicomponent plasmas, it may be useful to define $\Gamma_i = \Gamma_e \langle Z^{5/3} \rangle$.

The degeneracy parameter θ and the relativity parameter x are defined respectively as

$$\theta = T / T_F, \quad x = p_F / m_e c, \qquad (3)$$

where $T_F = (m_e c^2 / k_B) [\sqrt{1 + x^2} - 1] \approx (5.93 \times 10^9$ K$) [\sqrt{1 + x^2} - 1]$ is the Fermi temperature, c is the speed of light, and $p_F = \hbar (3 \pi^2 n_e)^{1/3}$ is the zero-temperature Fermi momentum of electrons. To estimate θ and x, it is useful to note that

$$x = \left(\frac{9 \pi}{4} \right)^{1/3} \frac{\alpha}{r_s} \approx \frac{0.014}{r_s} \approx \left(\frac{\langle Z \rangle}{\langle A \rangle} \frac{\rho}{10^6 \text{ g cm}^{-3}} \right)^{1/3}, \quad (4)$$

$$\theta = \frac{\alpha^2 (\Gamma_e r_s)^{-1}}{\sqrt{1 + x^2} - 1}, \quad \theta \approx 0.543 \frac{r_s}{\Gamma_e} \text{ at } x \ll 1, \qquad (5)$$

where $\alpha = 1/137.036$ is the fine-structure constant.

Various asymptotic expansions, interpolation formulas, and large tables have been derived in the past for the thermodynamic functions of free fermions (see Refs. [3,4] and references therein). In this paper, first, we present analytic expressions for the thermodynamic quantities of free fermions for arbitrary degeneracy and relativity, θ and x. Second,

we propose simple and accurate analytic approximations for the *nonideal* internal and free energies of the classical one-component plasma (OCP), which take into account the most recent hypernetted-chain (HNC) and Monte Carlo (MC) calculations by DeWitt, Slattery, and Chabrier [5] (DWSC) in the strong-coupling regime. Third, we consider the electron *screening* effects on the thermodynamic properties of the TCP. We employ a computational HNC scheme based on the linear screening theory with local-field corrections, taking into account the electron finite-temperature (finite-θ) effects. The numerical calculations have been performed over a wide range of Z, Γ_i, and r_s and interpolated by a simple analytic formula, which recovers the Debye-Hückel (DH) limit for the TCP at $\Gamma_i \ll 1$ and the Thomas-Fermi limit at large Γ_i and Z.

II. SUMMARY OF THE MODEL

Consider the Helmholtz free energy F, internal energy U, and pressure P of a TCP of N_i ions and N_e electrons in the volume V. The total free energy F_{tot} can be written as the sum of three terms

$$F_{\text{tot}} = F_{\text{id}}^{(i)} + F_{\text{id}}^{(e)} + F_{\text{ex}}, \tag{6}$$

where $F_{\text{id}}^{(i,e)}$ denote the ideal free energy of ions and electrons, respectively, and F_{ex} is the *excess* free energy arising from interactions.

In this paper we restrict ourselves to conditions where the ions behave classically, which is the case in most astrophysical situations. Quantum corrections for ions that can be important in the ultradense matter of white dwarf interiors, neutron stars, and supernova cores have been considered, e.g., in Refs. [6,7]. Thus $F_{\text{id}}^{(i)}$ is given by the Maxwell-Boltzmann expression. For $F_{\text{id}}^{(e)}$ we use the well-known expressions of the thermodynamic functions of the perfect gas of fermions (which may be degenerate and relativistic) through the generalized Fermi-Dirac integrals.

To calculate F_{ex}, we follow the model developed by Chabrier [8] for fully ionized EIPs. As long as the ion-electron interaction is weak compared to the kinetic energy of the electrons, $Ze^2/a_e \ll k_B T_F$, this interaction can be treated within the linear screening theory. Under these conditions, the exact Hamiltonian of the TCP can be separated out exactly into a Hamiltonian for the electron-screened ionic fluid and a Hamiltonian for a *rigid* electron background, the so-called jellium Hamiltonian H_e [9,10]:

$$H = H^{\text{eff}} + H_e, \tag{7}$$

with

$$H^{\text{eff}} = K_i + \frac{1}{2V} \sum_{\mathbf{k} \neq 0} \frac{4\pi(Ze)^2}{k^2} \left[\frac{\rho_{\mathbf{k}} \rho_{\mathbf{k}}^*}{\epsilon(k)} - N_i \right], \tag{8}$$

where K_i is the ionic kinetic (translational) term, $\rho_{\mathbf{k}}$ is the Fourier component of the ionic microscopic density, and $\epsilon(k)$ is the static screening function of the electron fluid to be discussed below. The Hamiltonian H^{eff} characterizes the electron-screened ion fluid with the interparticle potential whose Fourier transform is

$$V^{\text{eff}}(k) = \frac{4\pi(Ze)^2}{k^2 \epsilon(k)}, \tag{9}$$

which is the sum of the bare ionic potential and the induced polarization potential.

The ion-ion (ii) and the ion-electron (ie) Coulomb interactions can thus be separated from the exchange-correlation contribution in the electron fluid (ee). The excess part of the free energy (6) can then be written as $F_{\text{ex}} = F_{ee} + F_{ii} + F_{ie}$; the quantities labeled ie will be referred to as *electron-screening* quantities. It is convenient to consider dimensionless quantities $f_{ee} \equiv \beta F_{ee}/N_e$ and $f_{ii,ie} \equiv \beta F_{ii,ie}/N_i$. Then

$$f_{\text{ex}} = x_e f_{ee} + x_i (f_{ii} + f_{ie}), \tag{10}$$

where $x_{i,e} \equiv N_{i,e}/N$ denote the number fraction of ions and electrons, respectively, and $N = N_i + N_e$ is the total number of particles. In the same way we define $u_{ee} \equiv \beta U_{ee}/N_e$ and $u_{ii,ie} \equiv \beta U_{ii,ie}/N_i$. The excess free energy can be obtained from the internal energy by integration:

$$f_{\text{ex}}(\Gamma, r_s) = \int_0^{\Gamma} \frac{u_{\text{ex}}(\Gamma', r_s)}{\Gamma'} d\Gamma'. \tag{11}$$

For f_{ee}, we have adopted the interpolation formula of Ichimaru, Iyetomi, and Tanaka [11] (IIT), consistent with numerical results obtained by different authors. For f_{ii}, which corresponds to the well-known OCP model, that implies the rigid electron background ($\epsilon(k) = 1$), we present an analytic interpolation between the MC results [5] at $\Gamma_i \gtrsim 1$ and the DH limit and Abe correction at $\Gamma_i \lesssim 0.1$.

The ion-electron interactions are calculated numerically as in Ref. [8]. In this approach, the bare Coulomb potential in the expression for the electrostatic energy is replaced by the potential statistically screened by the electrons (9) and the HNC approximation is used to calculate the thermodynamic functions of the system. This model, originally applied to nonrelativistic hydrogen plasmas, is now extended to the case of arbitrary Z and x. In the nonrelativistic case ($x \ll 1$), the dielectric function $\epsilon(k)$ is the finite-temperature Lindhard function modified with the local-field correction arising from electron correlation effects.

At very high density, $x \gtrsim 1$, the electrons become relativistic. At such densities, the electron correlation effects are completely negligible. The finite-temperature effects ($\theta \neq 0$) may give an appreciable contribution to the screening part of the free energy f_{ie} only at extremely high temperatures, where the nonideality of the gas has no significance. Thus we use the Jancovici [12] zero-temperature dielectric function in the relativistic regime.

The correlation functions and thermodynamic quantities for the electron-screened ionic fluid are obtained within the framework of the HNC equations. The validity of the HNC theory for the Coulomb systems has been assessed by several authors by comparison with lengthy MC simulations. The HNC approximation consists of neglecting the contribution of the so-called bridge diagrams, which involves an infinite series of multiple integrals, in the N-body general diagrammatic resummations [13]. The long-range part of the direct correlation function $c(r)$ calculated within the HNC approximation is exactly canceled by $-V(r)/kT$, so that the pair

TABLE I. Parameters of Eqs. (18) and (19). The powers of 10 are given in square brackets.

i	1	2	3	4	5
$c_i^{(0)}$	0.37045057	0.41258437	$9.777982\,[-2]$	$5.3734153\,[-3]$	$3.8746281\,[-5]$
$c_i^{(1)}$	0.39603109	0.69468795	0.22322760	$1.5262934\,[-2]$	$1.3081939\,[-4]$
$c_i^{(2)}$	0.76934619	1.7891437	0.70754974	$5.6755672\,[-2]$	$5.5571480\,[-4]$
$\chi_i^{(0)}$	0.43139881	1.7597537	4.1044654	7.7467038	13.457678
$\chi_i^{(1)}$	0.81763176	2.4723339	5.1160061	9.0441465	15.049882
$\chi_i^{(2)}$	1.2558461	3.2070406	6.1239082	10.316126	16.597079
x_i	$7.265351\,[-2]$	0.2694608	0.533122	0.7868801	0.9569313
ξ_i	0.26356032	1.4134031	3.5964258	7.0858100	12.640801
h_i	$3.818735\,[-2]$	0.1256732	0.1986308	0.1976334	0.1065420
v_i	0.29505869	0.32064856	$7.3915570\,[-2]$	$3.6087389\,[-3]$	$2.3369894\,[-5]$

correlation function $g(r)$ is of much shorter range than the Coulomb potential $V(r)$ [13]. This is a required condition for Coulomb systems because of the perfect screening condition. This property of the HNC theory makes it particularly suitable for such long-range systems. The differences of the free energy, the internal energy, and the pressure are at most of the order of 1% (see, e.g., Refs. [5,8]). The difference is due to the lack of bridge functions in the HNC theory.

III. IDEAL PART OF THE FREE ENERGY

The ideal free energy of nonrelativistic classical ions, neglecting their spin statistics, reads [14]

$$F_{\mathrm{id}}^{(i)} = N_i k_B T[\ln(n_i \lambda_i^3) - 1], \tag{12}$$

where $\lambda_i = (2\pi\beta\hbar^2/m_i)^{1/2}$ is the thermal wavelength of ions. For electrons, we use the identity [14]

$$F_{\mathrm{id}}^{(e)} = N_e \mu_{\mathrm{id}}^{(e)} - P_{\mathrm{id}}^{(e)} V. \tag{13}$$

Here $\mu_{\mathrm{id}}^{(e)}$ is the chemical potential (in which we do not include the rest energy $m_e c^2$) and $P_{\mathrm{id}}^{(e)}$ is the pressure of the ideal Fermi gas. The pressure and number density, in turn, are functions of μ and T:

$$P_{\mathrm{id}}^{(e)} = \frac{(2m_e)^{3/2}}{3\pi^2\hbar^3\beta^{5/2}}\left(I_{3/2}(\chi,\tau) + \frac{\tau}{2}I_{5/2}(\chi,\tau)\right), \tag{14}$$

$$n_e = \frac{\sqrt{2}\,(m_e/\beta)^{3/2}}{\pi^2\hbar^3}(I_{1/2}(\chi,\tau) + \tau I_{3/2}(\chi,\tau)), \tag{15}$$

where $\tau = (\beta m_e c^2)^{-1} = T/5.93\times10^9$ K, $\chi = \beta\mu_{\mathrm{id}}^{(e)}$, and

$$I_\nu(\chi,\tau) \equiv \int_0^\infty \frac{x^\nu \sqrt{1+\tau x/2}}{\exp(x-\chi)+1}dx \tag{16}$$

is the generalized Fermi-Dirac integral.

In the limit $\tau\to0$, the Fermi-Dirac integrals reduce to the usual nonrelativistic Fermi integrals $I_\nu(\chi)$, which can be calculated using the highly accurate Padé approximations presented by Antia [15]. The chemical potential is obtained from the relationship

$$\chi = X_{1/2}(2\theta^{-3/2}/3), \tag{17}$$

where X_ν is the inverse Fermi integral, also fitted with high accuracy by Antia [15].

The accuracy of the nonrelativistic formulas decreases rapidly at $T>10^7$ K. Blinnikov et al. [3] have presented a number of approximations and asymptotic expansions of the relativistic thermodynamic functions of the ideal electron gas. We have selected those of their fitting formulas that are most accurate at low and moderate χ and supplemented them with asymptotic expansions at high χ to obtain an approximation that is accurate at any n_e for each of the Fermi integrals $I_\nu(\chi,\tau)$ with $\nu=\frac{1}{2}, \frac{3}{2}$, and $\frac{5}{2}$:

$$I_{k+1/2}(\chi,\tau) = \sum_{i=1}^5 c_i^{(k)}\frac{\sqrt{1+\chi_i^{(k)}\tau/2}}{\exp(-\chi_i^{(k)})+\exp(-\chi)} \quad (\chi\lesssim0.6) \tag{18}$$

$$= \sum_{i=1}^5\left[h_i x_i^k \frac{\chi^{k+3/2}\sqrt{1+\chi x_i\tau/2}}{1+\exp(\chi x_i-\chi)}\right.$$
$$\left. + v_i(\xi_i+\chi)^{k+1/2}\sqrt{1+(\xi_i+\chi)\tau/2}\right]$$
$$(0.6<\chi<14) \tag{19}$$

$$= F_k(\chi,\tau) + \frac{\pi^2}{6}\chi^k\frac{k+1/2+(k+1)\chi\tau/2}{R}$$
$$(\chi\gtrsim14), \tag{20}$$

where $R \equiv \sqrt{\chi(1+\chi\tau/2)}$,

$$F_0(\chi,\tau) = (\chi+\tau^{-1})R/2 - (2\tau)^{-3/2}\ln(1+\tau\chi+\sqrt{2\tau}\,R), \tag{21}$$

$$F_1(\chi,\tau) = [2R^3/3 - F_0(\chi,\tau)]/\tau, \tag{22}$$

$$F_2(\chi,\tau) = [2\chi R^3 - 5F_1(\chi,\tau)]/4\tau. \tag{23}$$

If $\chi\tau\ll1$, the functions $F_k(\chi,\tau)$ should be replaced by their nonrelativistic limits $\chi^{k+3/2}/(k+3/2)$. The constants $c_i^{(k)}$, $\chi_i^{(k)}$, x_i, ξ_i, h_i, and v_i are adopted from Ref. [3] and are listed in Table I. The relative error of the approximation (18)–(20) does not exceed 0.2% at $\tau\lesssim10^2$ (any χ), being typically a few parts in 10^4.

The chemical potential $\mu_{\mathrm{id}}^{(e)}$ can be obtained numerically from Eq. (15), using Eqs. (18)–(20). We have constructed also an analytic fit to χ:

$$\chi = \chi^{\mathrm{nonrel}} - \frac{3}{2}\ln\left[1 + \left(\frac{\tau}{1+\tau/2\theta}\right)\frac{1+q_1\sqrt{\tau}+q_2q_3\tau}{1+q_2\tau}\right].$$
(24)

Here χ^{nonrel} is given by the nonrelativistic formula (17) and the coefficients q_i are functions of θ:

$$q_1 = \frac{3}{2}(e^\theta - 1)^{-1},$$

$$q_2 = 12 + 8\theta^{-3/2},$$

$$q_3 = \frac{2}{\pi^{1/3}} - \frac{e^{-\theta} + 1.612e^\theta}{6.192\theta^{0.0944}e^{-\theta} + 5.535\theta^{0.698}e^\theta}.$$

The relative error $\delta\chi/\chi$ becomes infinite at $\chi = 0$. However, since thermodynamic quantities are expressed through χ by virtue of thermal averaging of type of Eq. (16), a natural measure of the error is $\delta\chi/\max(|\chi|,1) = \delta\mu/\max(|\mu|,k_BT)$. The error thus lies within 0.4% for $\tau > 1$ and is smaller than 0.2% if $\tau < 1$ (any θ). Another measure of the accuracy is the relative difference between the densities n_e calculated with the exact and fitted values of μ. This difference lies within 0.4% for $\tau \gtrsim 1$ and within 0.1% for $\tau < 1$.

This accuracy may not be sufficient for calculation of temperature derivatives of the electron-gas equation of state (EOS) (heat capacity, temperature exponent, etc.) in the regime of strong degeneracy ($\chi \gg 1$). In this case, however, Sommerfeld asymptotic expansions for these quantities may be used (see, e.g., Ref. [16]). In this paper we do not consider the positrons, which are efficiently created at $\tau \gtrsim 1$ (see Ref. [3] for a description of the equilibrium electron-positron plasma).

IV. OCP LIQUID OF CLASSICAL IONS

Liquid and solid phases of the OCP have been studied extensively by various numerical methods, MC simulations, or N-body semianalytic theories such as the HNC theory (see Refs. [17,11] for detailed reviews). All the thermodynamic functions of the OCP of classical ions in a uniform (rigid) electron background can be expressed as functions of the only parameter Γ_i. The melting point of the OCP corresponds to $\Gamma_i \approx 172$, above which it forms a Coulomb crystal [18]. The most accurate MC and HNC results for the internal and free energies of the liquid OCP for $1 \le \Gamma_i \le 160$ have been obtained recently by DWSC [5] (see references therein for earlier results). The high precision of the calculations allowed the authors to investigate the tiny effects of nonadditivity of the excess energy of binary ionic mixtures, as will be discussed in Sec. VI.

DWSC have also derived a highly accurate analytic fit to the MC simulations of the internal energy of the OCP in the aforementioned Γ range:

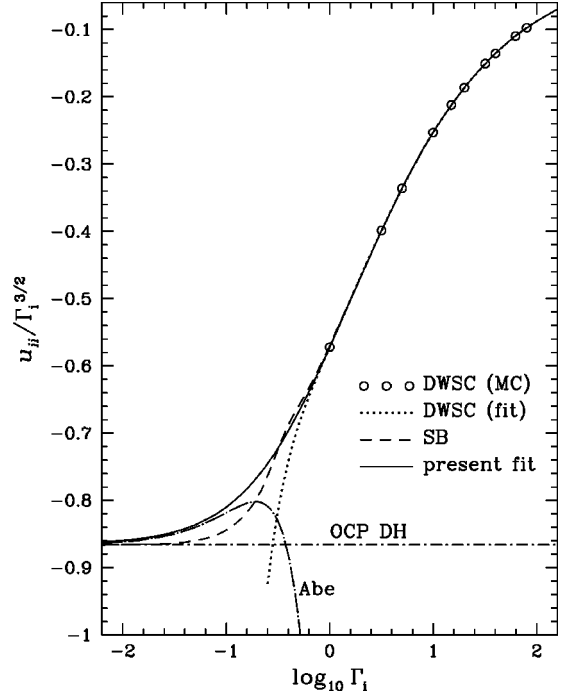$$u_{ii} = a\Gamma_i + b\Gamma_i^s + c,$$
(25)

FIG. 1. Comparison of the fit (solid line) given by Eq. (27) for the OCP internal energy with the DH and Abe asymptotic expansions at small Γ_i (dot-dashed lines) and with the DWSC results [5] at $1 \le \Gamma_i \le 160$ (dots and circles). The dashed curve represents the interpolation of SB [22].

with $a = -0.899\,126$, $b = 0.607\,12$, $c = -0.279\,98$, and $s = 0.321\,308$. The maximum relative difference between calculated and fitted values reaches 17 parts in 10^5 at $\Gamma_i = 3.1748$.

Equation (25), however, does not apply to the weak-coupling region $\Gamma_i < 1$. At very small Γ_i, the internal energy of the OCP must recover the well-known DH expression $u_{ii} = -(\sqrt{3}/2)\Gamma_i^{3/2}$, whereas at moderately small Γ_i this limit must include the Abe correction [19]

$$u_{ii} = -\frac{\sqrt{3}}{2}\Gamma_i^{3/2} - 3\Gamma_i^3\left[\frac{3}{8}\ln(3\Gamma_i) + \frac{\gamma}{2} - \frac{1}{3}\right],$$
(26)

where $\gamma = 0.577\,21\ldots$ is Euler's constant.

We represent the internal energy of the ionic fluid ($\Gamma_i \lesssim 170$) by a simplified version of the fitting formula proposed by Hansen [20,21],

$$u_{ii} = \Gamma_i^{3/2}\left[\frac{A_1}{\sqrt{A_2+\Gamma_i}} + \frac{A_3}{1+\Gamma_i}\right],$$
(27)

where A_1 and A_2 are fitting parameters and $A_3 = -\sqrt{3}/2 - A_1/\sqrt{A_2}$. We have found that the minimum relative difference between Eq. (27) and the MC results of DWSC [5], smaller than 6 parts in 10^4, is obtained with $A_1 = -0.9052$ and $A_2 = 0.6322$. This accuracy is sufficient for our present study since it is much better than the available numerical accuracy of the complementary contribution to the internal energy u_{ie}. As mentioned in Sec. II, the HNC calculations of the *sum* $u_{ii} + u_{ie}$ ensure an accuracy of the order of 1%.

Figure 1 presents a comparison of our interpolation for-

mula (27) with the DH-Abe formulas, the MC results and the fit (25) of DWSC [5], and the interpolation proposed by Stolzmann and Blöcker [22] (SB) following Ebeling [23]. Unlike SB, our Eq. (27) accurately reproduces Eq. (26) in the range $\Gamma_i \sim 0.01 - 0.1$ and provides a smoother transition between the strong- ($\Gamma_i > 1$) and weak- ($\Gamma_i \lesssim 1$) coupling regimes.

Using Eqs. (27) and (11), we obtain the Helmholtz free energy (cf. Ref. [20])

$$f_{ii}(\Gamma_i) = A_1 [\sqrt{\Gamma_i(A_2 + \Gamma_i)} - A_2 \ln(\sqrt{\Gamma_i/A_2} + \sqrt{1 + \Gamma_i/A_2})]$$
$$+ 2A_3 [\sqrt{\Gamma_i} - \arctan(\sqrt{\Gamma_i})]. \quad (28)$$

At $\Gamma_i \gtrsim 1$, this formula gives f_{ii}, which differs from the HNC calculations and the fit of DWSC [5] by no more than 0.8%. This difference approximately coincides with that between the MC and HNC results for u_{ii}; therefore, it should be attributed to the lack of the bridge functions in the HNC approximation (see Sec. II). On the other hand, Eq. (28) recovers the DH-Abe free energy with an error smaller than 0.6% at $\Gamma_i < 0.1$.

V. ELECTRON FLUID

The exchange and correlation effects in electron fluid were studied by many authors. For instance, Tanaka et al. [24] calculated the interaction energy of the electron fluid at finite temperature in the Singwi-Tosi-Land-Sjölander [25] approximation and presented a fitting formula that reproduces their results as well as various exact limits with digressions less than 1% (in particular, their formula incorporates the parametrization of the exchange energy by Perrot and Dharma-wardana [26]). We adopt a modification of this formula given by IIT [11].

The exchange-correlation free energy f_{ee} is obtained by integration from Eq. (11). It is important to note that Tanaka et al. [24] give a fit to the *interaction* energy of the electron fluid but not to the thermodynamic *internal* energy (the quantities differ at finite θ). This enabled Tanaka et al. to obtain f_{ee} by integration of their fitting formula over Γ_e at constant θ (the integration of the internal energy would have to be performed at constant r_s). Note also that the results of IIT are nonrelativistic.

More recently, SB [22] proposed other parametrizations of the exchange and correlation free energies. At moderate r_s, a comparison of the formulas given by SB and IIT reveals only small differences, which do not exceed the uncertainty in the various numerical results found in the literature [26,27]. Unlike IIT, SB evaluated the exchange energy at $\theta < 1$ in the relativistic case. On the other hand, the SB fit reaches the classical OCP limit at large r_s and moderate Γ_e with digressions up to 4.4%, while the parametrization of IIT is several times more accurate in this limit. We shall use the IIT's formula hereafter.

VI. ELECTRON SCREENING

A. Numerical calculations

In order to calculate the screening contribution, we have employed the model of Ref. [8], outlined in Sec. II. The HNC equations were solved numerically for the effective
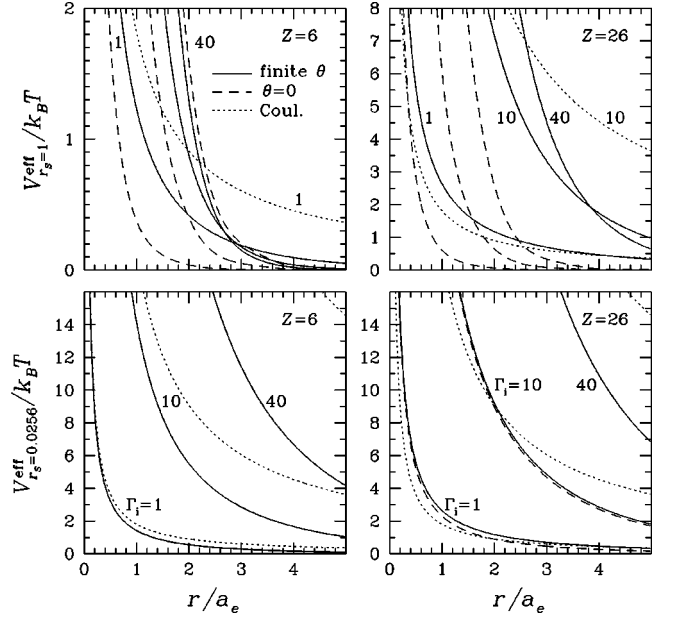

FIG. 2. Effective ion-ion potentials V^{eff} at various approximations for $Z = 6$ (left panels) and $Z = 26$ (right panels), for two densities, $r_s = 1$ (upper panels) and 0.0256 (lower panels) and three values of $\Gamma_i = 1$, 10, and 40. Solid lines represent the finite temperature V^{eff} including the local-field correction and dashed lines show the zero-temperature RPA (the dashed and solid lines practically coincide on the lower left panel). The bare Coulomb potential is drawn by dots for comparison.

screened interionic potential (9) to obtain $f_{ii} + f_{ie}$, $u_{ii} + u_{ie}$ and $P_{ii} + P_{ie}$ and for the bare Coulomb potential to obtain f_{ii}, u_{ii}, and P_{ii}. The difference represents the screening (*ie*) contribution to the thermodynamic quantities.

The previous numerical results [8] have been obtained for the hydrogen plasma ($Z = 1$). We extend the calculations to different values of Z and a larger set of r_s. Figure 2 shows the effective potentials V^{eff} for $Z = 6$ and $Z = 26$ at several values of r_s, compared with the bare Coulomb potential and with V^{eff} in the zero-temperature ($\theta = 0$) random-phase approximation (RPA) (no local-field correction). One can see that the latter approximation works well at the small value of $r_s = 0.0256$ (lower panels), while it breaks down completely at $r_s = 1$ (upper panels).

The bulk of the calculations has been performed in the nonrelativistic approximation, for 13 ion charges from $Z = 1$ to $Z = 26$ listed in the first column of Table II, at ten values of the density parameter r_s ranging from $r_s = 0.0256$ to $r_s \approx 2$, and, at each Z and r_s, for several tens of values of the coupling parameter Γ_i that range from the DH limit at $\Gamma_i = 0.001$ to $\Gamma_i \sim 200$. As an example, calculated values of the normalized screening part of the free energy f_{ie} at $Z = 6$ are shown by filled circles in Fig. 3. Note that it is the account of the finite electron temperature in the dielectric function that allows us to reach the correct TCP DH limit at low values of Γ_i (see Ref. [8]).

In order to supplement the aforementioned nonrelativistic data at higher densities, we have also performed calculations using the Jancovici [12] zero-temperature dielectric function. The results are shown in Fig. 3 for $\Gamma_i \gtrsim 1$ and $r_s = 0.0625$ ($x = 0.224$), 0.0256 ($x = 0.545$), and 0.008 (x

TABLE II. Root mean square and maximum relative differences between the fit and the HNC calculations for $f_{ii}+f_{ie}$, $u_{ii}+u_{ie}$, and $P_{ii}+P_{ie}$; the bottom line corresponds to the OCP model.

Z	$(\delta f/f)$ (%)		$(\delta u/u)$ (%)		$(\delta P/P)$ (%)	
	rms	max	rms	max	rms	max
1	0.6	1.9	0.9	1.8	1.2	4.5
2	0.4	1.1	0.7	1.8	0.7	3.0
3	0.4	0.8	0.9	2.3	0.7	1.8
4	0.5	1.2	1.3	3.1	0.9	1.9
5	0.6	1.5	1.6	3.9	1.2	2.4
6	0.7	1.8	1.8	4.3	1.5	2.8
7	0.6	1.7	1.9	4.6	1.7	3.5
8	0.7	1.5	1.9	4.6	1.9	4.1
10	0.6	1.2	1.8	3.9	2.0	4.1
12	0.5	1.2	1.6	3.2	1.9	4.5
14	0.5	1.2	1.9	4.5	1.6	3.2
20	0.5	1.1	1.2	2.8	1.8	4.5
26	0.6	1.7	1.2	2.6	1.3	3.8
OCP	0.6	0.7	0.6	0.8	0.6	0.8

$=1.75$). A comparison for the case of $r_s=0.0625$ confirms that the zero-temperature approximation works well at small r_s and large Γ [where $\theta \ll 1$ due to the relation (5)]; this conclusion is corroborated by inspection of Fig. 2.

Thus the numerical results cover all values of r_s and Γ (i.e., ρ and T) that are relevant for liquid EIPs. At $r_s \gtrsim 1$ and $\Gamma_i \gtrsim 1$, the formation of bound states sets in. At $r_s \lesssim 10^{-2}$ and $\Gamma_i \lesssim 1$, the temperature reaches the values
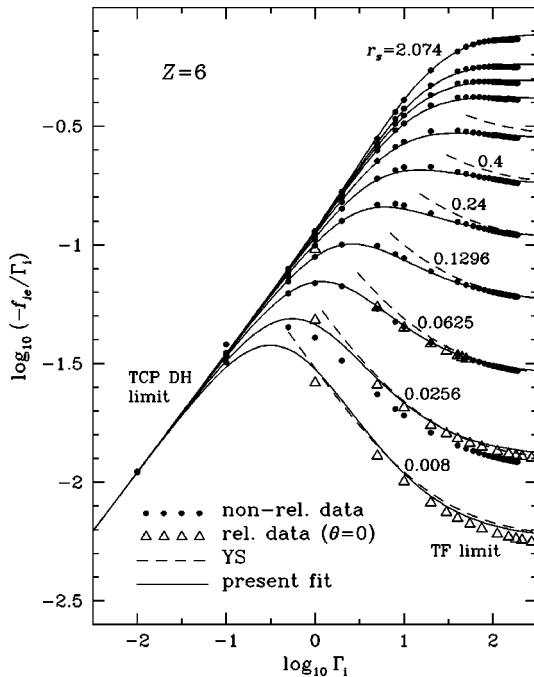

FIG. 3. Nonrelativistic finite-temperature (filled circles) and relativistic zero-temperature (open triangles) calculated values of the screening part f_{ie} of the free energy of the TCP for $Z=6$, compared with the fit (29) (solid lines). The fit is also compared with the approximation of YS [16] (dashed line), which is valid at small r_s and large Γ_i. TF denotes the Thomas-Fermi approximation.

$T \gtrsim 3 \times 10^7 Z^{5/3}$ K, where the electron screening effects are completely unimportant. Finally, at $\Gamma_i \gtrsim 170$, solidification takes place.

B. Analytic formulas

The calculated values of the screening free energy are fitted by the following function of r_s, Γ_e, and Z:

$$f_{ie}=-\Gamma_e \frac{c_{DH}\sqrt{\Gamma_e}+c_{TF}a\Gamma_e^{\nu}g_1(r_s)h_1(x)}{1+[b\sqrt{\Gamma_e}+ag_2(r_s)\Gamma_e^{\nu}/r_s]h_2(x)}. \quad (29)$$

The parameter

$$c_{DH}=\frac{Z}{\sqrt{3}}[(1+Z)^{3/2}-1-Z^{3/2}] \quad (30)$$

ensures transition to the DH value of the excess free energy of the EIP, $f_{ex}^{DH}=-Z[(1+Z)/3]^{1/2}\Gamma_e^{3/2}$ at small Γ_e. The parameter

$$c_{TF}=c_{\infty}Z^{7/3}(1-Z^{-1/3}+0.2Z^{-1/2}) \quad (31)$$

determines the screening in the limit of large Γ_e and small r_s. The parameter $c_{\infty}=(18/175)(12/\pi)^{2/3}=0.2513$ is consistent with the Thomas-Fermi approximation [28], which becomes exact at small r_s and very large Z (cf. Ref. [16]). The parameters

$$a=1.11Z^{0.475},$$

$$b=0.2+0.078(\ln Z)^2,$$

$$\nu=1.16+0.08\ln Z$$

provide a low-order approximation to f_{ie} (with a maximum error up to 30% at large Z and $r_s \gtrsim 1$), while the functions

$$g_1(r_s)=1+\frac{0.78}{21+\Gamma_e(Z/r_s)^3}\left(\frac{\Gamma_e}{Z}\right)^{1/2}, \quad (32)$$

$$g_2(r_s)=1+\frac{Z-1}{9}\left(1+\frac{1}{0.001Z^2+2\Gamma_e}\right)\frac{r_s^3}{1+6r_s^2} \quad (33)$$

improve the fit at relatively large r_s and reduce the maximum fractional error in f_{ie} to 4.3% and the root-mean-square (rms) error to $\sim 1.5\%$. The factors $h_1(x)=[1+(v_F/c)^6 Z^{-1/3}]^{-1}$ (where $v_F=cx/\sqrt{1+x^2}$ is the electron Fermi velocity) and $h_2(x)=(1+x^2)^{-1/2}$ are relativistic corrections and may be omitted at $x \ll 1$.

Note that f_{ie} constitutes only a part of the ion excess free energy $f_{ii}+f_{ie}$. The fit to this latter quantity is given by the sum of Eqs. (28) and (29). The second and third columns of Table II present the rms and maximum relative differences between the calculated and fitted values of $f_{ii}+f_{ie}$ at each value of Z. The comparison has been done for the set of finite-temperature numerical results at $0.1 \leqslant \Gamma_i \leqslant 170$ and $0.0625 \leqslant r_s \leqslant 2.074$. The remaining four columns of the table present the rms and maximum relative differences for the $(ii+ie)$ internal energy and pressure, derived from the fits by the use of the thermodynamic relations
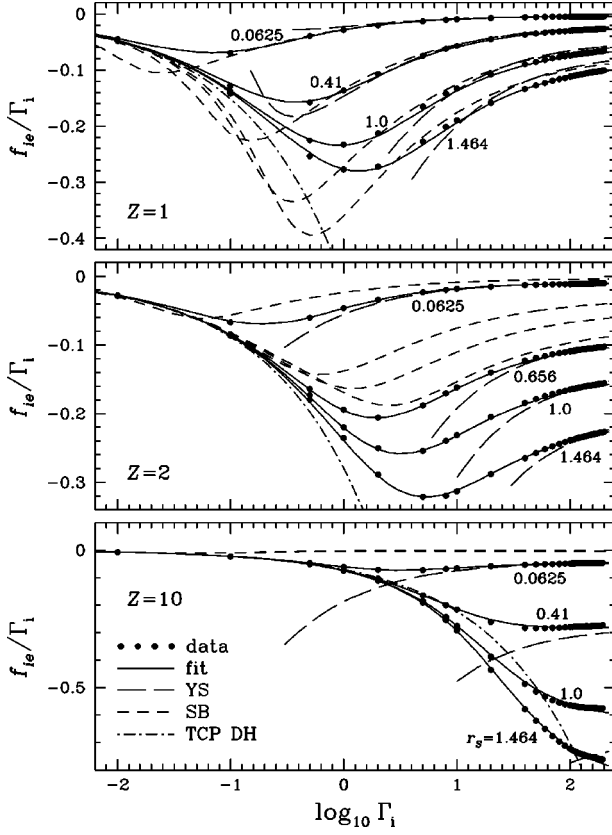
FIG. 4. Calculated (filled circles) and fitted (solid line) f_{ie} for $Z = 1$, 2, and 10, for several indicated values of r_s, compared with the approximations of DH (dot-dashed lines), YS (long-dashed lines), and SB (short-dashed lines).

$$u = \left(\frac{\partial f}{\partial \ln \Gamma} \right)_{r_s}, \quad \beta P/n = \frac{1}{3} \left[u - \left(\frac{\partial f}{\partial \ln r_s} \right)_{\Gamma} \right]. \quad (34)$$

The bottom row of the table is given for reference and presents the difference between the fit (28) and numerical HNC data in the OCP model (i.e., without the *ie* contribution).

The calculated and fitted values of f_{ie} are shown in Fig. 3 for $Z = 6$ and in Fig. 4 for $Z = 1, 2,$ and 10. For comparison, we have plotted the fit of Yakovlev and Shalybkov [16] (YS) to their relativistic calculations, carried out in the zero-temperature approximation (justified at small r_s and large Γ_e). In Fig. 4 we have also plotted f_{ie} given by an analytic expression of Ebeling *et al.* [29] reproduced by SB [22]. For the hydrogen plasma ($Z = 1$) it reproduces the Padé approximations of Ref. [30]. One can see that the fit of YS, in the range of its validity, agrees with our results. On the contrary, the approximation of Refs. [29,22] is clearly invalid in most cases. It exhibits unphysical behavior around $\Gamma_i \sim 0.1$, predicting an enhancement of screening with decreasing r_s (e.g., for $Z = 1$ and $\Gamma_i = 0.1$ it gives larger f_{ie} at $r_s = 0.41$ than at $r_s = 1.464$). Moreover, the extrapolation to $Z > 1$, proposed in Ref. [29], severely underestimates the screening effects.

Figure 5 exhibits an analogous comparison for the excess free energy (10) for $Z = 1$. We have also plotted the Padé approximation of IIT [11]. Although the digressions between the fit and numerical data of Ref. [11] lie within 0.4%, there
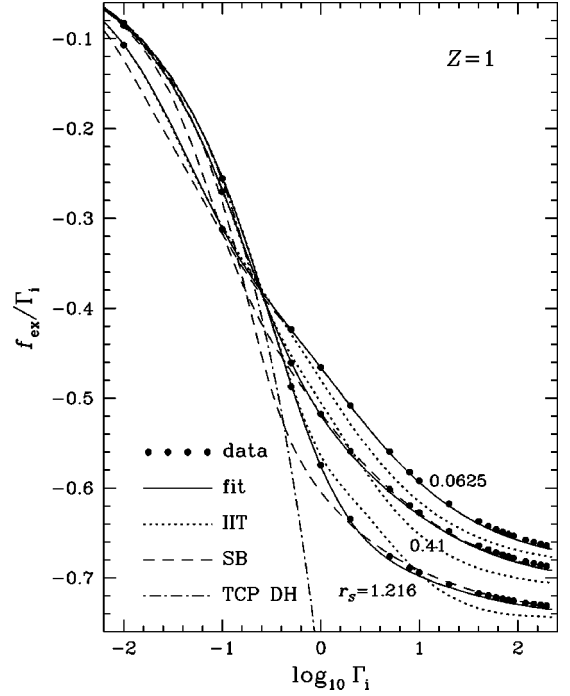

FIG. 5. Calculated (filled circles) and fitted (solid lines) excess free energy $f_{ex} = x_i(f_{ii} + f_{ie}) + x_e f_{ee}$ for $Z = 1$ for different values of the density parameter r_s. The dot-dashed line is the DH formula, while the dashed and dotted lines represent the approximations of SB [22] and IIT [11], respectively.

are significant deviations between IIT's fit and our present results. This discrepancy originates from the relatively small number of numerical calculations used by IIT (32 computed values at $0.1 \leqslant \Gamma_i \leqslant 10$ and $0.1 \leqslant \theta \leqslant 10$). Our fit, based on a much larger set of numerical data, reproduces not only these data but also the numerical results of IIT [11].

The excess ionic pressure $P_{ii} + P_{ie}$ is shown in Fig. 6. Calculated data are compared with the pressure obtained by differentiation (34) of our fit and of SB's fit. The DH approximation, shown for reference, is calculated as the difference between the DH pressures of the electron-ion TCP and the electron OCP. The importance of the screening effects is verified by a comparison of our calculated and fitted pressure with the pressure of the OCP in the rigid background P_{ii}, also shown in the figure.

Figure 7 demonstrates the validity of the EOS derived from our analytic formulas. The EOS of the perfect ion-electron gas is compared with the EOS that includes the non-ideality of the electron and ion fluids but neglects the *ie* interactions; solid lines show the complete EOS. The gaps in some isotherms indicate the regions where the formation of bound states could not be neglected. The significant deviations of the broken lines from the full lines in certain ranges of ρ and T demonstrate the importance of the *ion-electron* screening effects.

VII. MULTI-IONIC MIXTURES

The multi-ionic mixture is a straightforward generalization of the previous single-ion model. In that case the effective Hamiltonian (8) reads
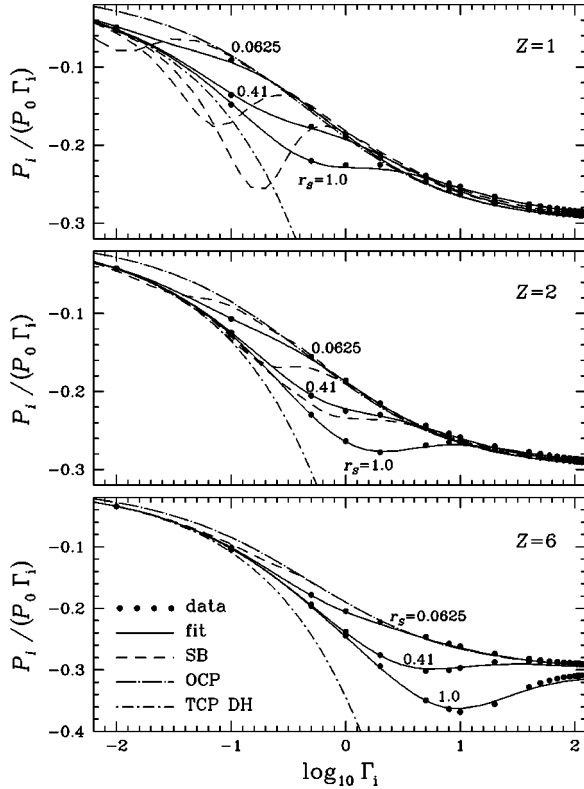
FIG. 6. Calculated (filled circles) and fitted (solid lines) excess pressure of ions in the compressible electron background, $P_i = P_{ii} + P_{ie}$, in units of $P_0 \Gamma_i$, where $P_0 = n_i k_B T$. For comparison, SB's approximation is shown by dashed lines and the DH and OCP approximations are shown by dot-dashed lines.

$$H^{\text{eff}} = K_i + \frac{1}{2V} \sum_{\mathbf{k} \neq \mathbf{0}} \frac{4\pi e^2}{k^2} \left[\frac{\rho_{Z\mathbf{k}} \rho_{Z\mathbf{k}}^*}{\epsilon(k)} - N_i \langle Z^2 \rangle \right], \quad (35)$$

where $\rho_{Z\mathbf{k}} = \Sigma_i Z_i \rho_{i\mathbf{k}}$ are the Fourier components of the ion charge number fluctuations.

For the binary ionic mixture in a rigid electron background $[\epsilon(k) = 1 \ \forall k]$, the excess (nonideal) free energy of the mixture, as well as the related thermodynamic quantities, can be expressed with high accuracy by the so-called linear mixing rule (LMR) in terms of the free energy of the pure phases

$$f_{\text{ex}}(Z_1, Z_2, \Gamma_e, x_1) \approx x_1 f_{\text{ex}}(\Gamma_1, x_1 = 1)$$
$$+ (1 - x_1) f_{\text{ex}}(\Gamma_2, x_1 = 0), \quad (36)$$

where $\Gamma_i = \Gamma_e Z_i^{5/3}$ and $x_1 = N_1 / (N_1 + N_2)$. The very high level of accuracy of the LMR (36) was demonstrated by Hansen *et al.* [21] and confirmed later on by several authors, using very accurate MC calculations (see, e.g., [5,31]).

The validity of the LMR in the case of an ionic mixture immersed in a *responsive* finite-temperature electron background, as described by the Hamiltonian (35), has been examined by Hansen *et al.* [21] in the first-order thermodynamic perturbation approximation and more recently by Chabrier and Ashcroft [32], who have solved the HNC equations with the effective screened potentials for arbitrary charge ratios ranging from a symmetric case $(Z_2/Z_1 \sim 1)$ to
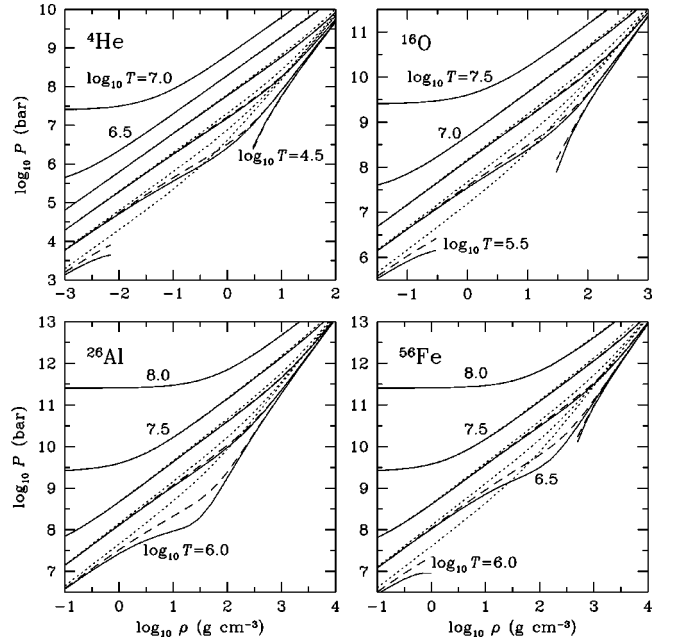

FIG. 7. Equations of state (EOSs) of fully ionized plasmas of four elements ($Z = 4$, 8, 13, and 26) given by the present analytic approximations. Solid lines show the pressure P vs density ρ taking into account the nonideality effects; dots represent the EOS of the perfect gas of ions and electrons; dashes display an EOS in which the electron-ion screening effects are neglected. The gaps in some isotherms indicate the regions where the formation of bound electron states can be expected.

a highly asymmetric case $(Z_2/Z_1 \gg 1)$. These authors found that the LMR remains valid to a high degree of accuracy when the electron response is taken into account in the interionic potential, except possibly for highly asymmetric mixtures in the region of weak degeneracy of the electron gas (where the departure from linearity can reach a few percent).

VIII. CONCLUSIONS

We have developed a completely analytic model for the free energy of fully ionized electron-ion Coulomb plasmas. The ideal part of the free energy of electrons and ions is described by Eqs. (12)–(15) and is accurately represented by the analytic fits given by Eqs. (18)–(24). Note that these formulas provide the thermodynamic quantities of a free electron gas for *any* degeneracy and relativity. For the excess free energy of the electron fluid at finite temperature, we adopt the analytic approximation from Ref. [11]. For the excess free energy of the classical ionic OCP, we provide a simple interpolation (28) that accurately reproduces the Monte Carlo results at $\Gamma_i \gtrsim 1$ and the Debye-Hückel–Abe limit for $\Gamma_i \lesssim 1$. Finally, we have taken into account the ion-electron interactions by solving the hypernetted-chain equations for a large set of the parameters Γ_i, r_s, and Z and constructed an analytic fit given by Eq. (29). Our analytic formulas reproduce $f_{ii} + f_{ie}$ with accuracy ~ 1–2 % and the derivatives of this function with respect to r_s and Γ_i give an excess internal energy and pressure with relative errors not larger than a few percent. This analytic approximation is significantly more accurate than previous approximations of the free energy of the electron-ion plasmas.

As mentioned in the Introduction, our calculations imply full ionization, i.e., pointlike ions from which their bound electrons are stripped completely. This model is realistic in various conditions at high temperatures or densities encountered in modern laser experiments and in various astrophysical situations, for example, stellar, brown dwarf, and giant planet interiors or the envelopes of neutron stars. In these situations, complete ionization can be safely assumed. Furthermore, the present model can be used as the basis of more elaborate equations of state aimed at describing the thermo-dynamic properties of partially ionized plasmas and ionization equilibrium. Work in this direction is in progress.

[1] Reviews are given, for example, in *The Equation of State in Astrophysics*, edited by G. Chabrier and E. Schatzman (Cambridge University Press, Cambridge, 1994).

[2] See, e.g., D. Saumon and G. Chabrier, Phys. Rev. A **46**, 2084 (1992); D. Saumon, G. Chabrier, and H. M. Van Horn, Astrophys. J., Suppl. Ser. **99**, 713 (1995), and references therein.

[3] S. I. Blinnikov, N. V. Dunina-Barkovskaya, and D. K. Nadyozhin, Astrophys. J., Suppl. Ser. **106**, 171 (1996).

[4] J. A. Miralles and K. A. Van Riper, Astrophys. J., Suppl. Ser. **105**, 407 (1996).

[5] H. DeWitt, W. Slattery, and G. Chabrier, Physica B **228**, 158 (1996).

[6] G. Chabrier, Astrophys. J. **414**, 695 (1993).

[7] M. D. Jones and D. M. Ceperley, Phys. Rev. Lett. **76**, 4572 (1996).

[8] G. Chabrier, J. Phys. (Paris) **51**, 1607 (1990).

[9] S. Galam and J. P. Hansen, Phys. Rev. A **14**, 816 (1976).

[10] N. W. Ashcroft and D. Stroud, Solid State Phys. **33**, 1 (1978).

[11] S. Ichimaru, H. Iyetomi, and S. Tanaka, Phys. Rep. **149**, 91 (1987).

[12] B. Jancovici, Nuovo Cimento **25**, 428 (1962).

[13] J. P. Hansen and I. R. McDonald, *Theory of Simple Liquids* (Academic, New York, 1976).

[14] L. D. Landau and E. M. Lifshitz, *Statistical Physics, Part I* (Pergamon, Oxford, 1986).

[15] H. M. Antia, Astrophys. J., Suppl. Ser. **84**, 101 (1993).

[16] D. G. Yakovlev and D. A. Shalybkov, Sov. Sci. Rev. Sect. E **7**, 311 (1989).

[17] M. Baus and J. P. Hansen, Phys. Rep. **59**, 1 (1980).

[18] H. Nagara, Y. Nagata, and T. Nakamura, Phys. Rev. A **36**, 1859 (1987).

[19] R. Abe, Prog. Theor. Phys. **21**, 475 (1959).

[20] J. P. Hansen, Phys. Rev. A **8**, 3097 (1973).

[21] J. P. Hansen, G. M. Torrie, and P. Vieillefosse, Phys. Rev. A **16**, 2153 (1977).

[22] W. Stolzmann and T. Blöcker, Phys. Lett. A **221**, 99 (1996); Astron. Astrophys. **314**, 1024 (1996).

[23] W. Ebeling, Contrib. Plasma Phys. **30**, 553 (1990).

[24] S. Tanaka, S. Mitake, and S. Ichimaru, Phys. Rev. A **32**, 1896 (1985).

[25] W. L. Singwi, M. P. Tosi, R. H. Land, and A. Sjölander, Phys. Rev. **176**, 589 (1968).

[26] F. Perrot and C. Dharma-wardana, Phys. Rev. A **30**, 2619 (1984).

[27] M. A. Pokrant, Phys. Rev. A **16**, 413 (1977); R. D. Dandrea, N. W. Ashcroft, and A. E. Carlsson, Phys. Rev. B **34**, 2097 (1986).

[28] E. E. Salpeter, Astrophys. J. **134**, 669 (1961).

[29] W. Ebeling, A. Förster, V. E. Fortov, V. K. Gryaznov, and A. Ya. Polishchuk, *Thermophysical Properties of Hot Dense Plasmas* (Teubner, Stuttgart, 1991).

[30] W. Ebeling and W. Richert, Phys. Status Solidi B **128**, 467 (1985).

[31] Y. Rosenfeld, Phys. Rev. E **52**, 3292 (1995); **54**, 2827 (1996).

[32] G. Chabrier and N. W. Ashcroft, Phys. Rev. A **42**, 2284 (1990).